Biochemistry

 Volume 39, Number 25 June 27, 2000

Accelerated Publications

Structural Similarities between MutT and the C-Terminal Domain of MutY†

David E. Volk,‡ Paul G. House,§ Varatharasa Thiviyanathan,‡ Bruce A. Luxon,‡ Shanmin Zhang,‡ R. Stephen Lloyd,§ and David G. Gorenstein*,‡

Sealy Center for Structural Biology and Sealy Center for Molecular Sciences, Department of Human Biological Chemistry and Genetics, University of Texas Medical Branch, 301 University Boulevard, Galveston, Texas 77555

Received February 23, 2000; Revised Manuscript Received April 18, 2000

ABSTRACT: One of the functions of MutY from *Escherchia coli* is removal of adenine mispaired with 7,8-dihydro-8-oxoguanine (8-oxoG), a common lesion in oxidatively damaged DNA. MutY is composed of two domains: the larger N-terminal domain (p26) contains the catalytic properties of the enzyme while the C-terminal domain (p13) affects substrate recognition and enzyme turnover. On the basis of sequence analyses, it has been recently suggested that the C-terminal domain is distantly related to MutT, a dNTPase which hydrolyzes 8-oxo-dGTP [Noll et al. (1999) *Biochemistry 38*, 6374−6379]. We have studied the solution structure of the C-terminal domain of MutY by NMR and find striking similarity with the reported solution structure of MutT. Despite low sequence identity between the two proteins, they have similar secondary structure and topology. The C-terminal domain of MutY is composed of two α-helices and five β-strands. The NOESY data indicate that the protein has two β-sheets. MutT is also a mixed α/β protein with two helices and two β-sheets composed of five strands. The secondary structure elements are similarly arranged in the two proteins.

Oxidative damage to DNA has been implicated in mutagenesis, cancer, and aging (*1*). One of the most significant lesions produced by oxidative attack on DNA is 7,8-dihydro-8-oxoguanine (8-oxoG) (*2*). 8-oxoG is particularly mutagenic due to the propensity of some polymerases to pair it with adenine (*3*). In *Escherchia coli* a set of three enzymes, Fpg (MutM), MutY, and MutT, work in concert to combat the mutagenic properties of 8-oxoG (*4*, *5*). Fpg removes 8-oxoG paired with cytosine, and MutT hydrolyzes 8-oxo-dGTP so that it cannot be incorporated into DNA. MutY is a 39 kDa protein that catalyzes the removal of adenine mispaired with guanine, cytosine, 8-oxoG, and other lesions (*6*). *E. coli* strains deficient in MutY show elevated rates of G·C to T·A transversions (*7*). MutY homologues have been found in a number of species, and the sequence of the catalytic domain is conserved from *E. coli* to humans, indicating its fundamental significance in DNA repair (*8*). Proteolytic digestion revealed that MutY contains two domains (*9*, *10*): a 26 kDa N-terminal domain (approximately residues 1−225, p26) and a 13 kDa C-terminal domain (approximately residues 226−350, p13). The catalytic activity of the enzyme resides in the larger N-terminal domain. The structure of the N-terminal p26 domain has been solved by X-ray crystallography and shows that MutY belongs to the helix−hairpin−helix superfamily of base excision repair glycosylase and glycosylase/AP lyase enzymes (*11*). Crystals of the N-terminal p26 domain with adenine in the active site strongly suggest that MutY utilizes a base flipping mechanism (*11*).

† This work was supported by NIEHS (ES04091, GM59237, and ES06676), Welch Foundation (H-1296), and Sealy and Smith Foundation grants. The project was funded in part by an NIH fellowship to D.E.V. (T32 AI07536). Building funds for the UTMB NMR facility were provided by the NIH (1CO6CA59098). R.S.L. holds the Mary Gibbs Jones Distinguished Chair in Environmental Toxicology from the Houston Endowment.

* To whom correspondence should be addressed. Tel: 409-747-6800. Fax: 409-747-6850. E-mail: david@nmr.utmb.edu.

‡ Sealy Center for Structural Biology.

§ Sealy Center for Molecular Sciences.

10.1021/bi000416p CCC: $19.00
Published on Web 06/02/2000

Initial work studying the function of the C-terminal domain by comparing assays of intact MutY with the MutY N-terminal domain showed differences in activity and binding (*10*, *12*). More recently, larger differences have been demonstrated between intact MutY and the catalytic N-terminal domain in both the rate of excision of adenine and the rate of turnover after adenine excision from an A·8-oxoG mispair (*13*). This suggests that the C-terminal domain plays an important role in the specificity for A·8-oxoG (*13*). Noll et al. also suggest that the C-terminal domain of MutY is evolutionarily related to MutT, a pyrophosphohydrolase of 129 residues, despite ~12% identity. MutT prevents the incorporation of 8-oxo-dGTP by hydrolyzing it to 8-oxo-dGMP (*14*). Although the enzymes are involved in the catalysis of different chemical reactions, each recognizes 8-oxoG. The tertiary structure of MutT, determined by NMR,[1] is globular and compact with five β-strands and two α-helices with the parallel portion of the β-sheet sandwiched between the helices (*15*).

In this report on the structure of the p13 domain of MutY, we find striking similarities between the structure of MutT and that of the p13 domain of MutY. We present NMR evidence to show that the secondary structure and topology of the p13 domain of MutY are very similar to the reported structure of MutT.

MATERIALS AND METHODS

Cloning the MutY C-Terminal Domain. The region coding for the p13 domain, residues 226−350, of the *mutY* gene was PCR amplified from the vector pKKYEco (gift from Drs. J. H. Miller and M. L. Michaels) using primers designed with sequence information from the intact gene (*16*). Using restriction sites designed into the PCR primers, the coding region was inserted into the expression vector pET11a. The construct also coded for an added N-terminal methionine. This construct failed to produce significant amounts of the p13 protein. A recent study showed that, in some cases, increased expression of small proteins in *E. coli* was observed when single amino acid additions were made after the N-terminal methionine, particularly if the insertion was an arginine or lysine (*17*). On the basis of this work, the QuickChange (Stratagene) site-directed mutagenesis kit was used to insert a lysine between the codon for the added N-terminal methionine and the codon for glutamine 226. This addition is equivalent to including the last residue of the N-terminal p26 domain, lysine 225, with the p13 domain. Expression of the protein was significantly improved by the lysine addition. The protein being studied consisted of an N-terminal methionine and MutY residues 225−350 and will be referred to as Kp13.

Expression and Purification of ^{15}N- and ^{15}N−^{13}C-Labeled Kp13. An overnight culture of *E. coli* strain BL21(DE3) containing the Kp13 construct was grown in LB broth supplemented with 5 g/L glucose and 0.10 g/L ampicillin. The overnight culture was diluted 1:100 in minimal media (vida infra) and grown at 33 °C with vigorous shaking to an A_{600} of 0.35−0.45. One molar isopropyl β-D-thiogalactoside (IPTG) was added to a final concentration of 2 mM, and the culture was shaken at 33 °C for 6 h. The cells were collected by centrifugation (6500*g* for 10 min) at 4 °C and frozen at −80 °C.

Minimal media consisted of the following: 12 g/L Na_2HPO_4, 6 g/L KH_2PO_4, 2 mL/L 4.3 M NaCl, 2 mL/L of 1 M $MgSO_4$, 0.10 g/L ampicillin, 100 μL/L of 1 M $CaCl_2$, 2 g/L glucose (unlabeled or U-$^{13}C_6$ labeled), 1 g/L NH_4Cl (^{15}N labeled), 10 mL/L vitamin solution, and 1 mL/L trace metals solution. The vitamin solution consisted of the following: 10 mg of thiamin, 10 mg of niacinamide, 10 mg of pantothenic acid, 10 mg of pyridoxine hydrochloride, 10 mg of PABA, 1 mg of riboflavin, 10 mg of folic acid, and 10 mg of biotin. The vitamins were individually dissolved, combined, and made up to 100 mL total volume with H_2O. The following trace metals were combined, dissolved in 8 mL of concentrated HCl, and then brought to a final volume of 50 mL with H_2O: 0.69 g of $ZnCl_2$, 0.57 g of H_3BO_3, 0.25 g of $MnCl_2·4H_2O$, 0.184 g of $FeCl_2$, 80 mg of $CoCl_2$, 80 mg of $CuCl_2$, and 55 mg of $(NH_4)_6Mo_7O_{24}·4H_2O$.

Following the 6 h expression Kp13 was found to accumulate in the periplasm. To efficiently release the Kp13, the cells were subjected to an osmotic shock as follows. The frozen cell pellet was thawed at room temperature in 1× PBS and then resuspended with a homogenizer; the sample was centrifuged at 4 °C (6500*g* for 20 min), and the supernatant was discarded. The pellet was resuspended with a homogenizer in ice-cold 20% sucrose, and 5 mM Tris-HCl, pH 7.5, and incubated on ice for 30 min. The sample was centrifuged at 4 °C (6500*g* for 20 min), the supernatant was discarded, and the pelleted cells were resuspended with a homogenizer in ice-cold autoclaved water and incubated on ice for 30 min. The sample was centrifuged at 4 °C (6500*g* for 20 min), and the supernatant which should primarily contain soluble proteins from the periplasm was collected. An equal volume of room temperature saturated $(NH_4)_2SO_4$ solution was added to the collected supernatant with stirring. This solution was incubated on ice for 30 min and then centrifuged at 4 °C (6500*g* for 20 min). The supernatant was discarded, and the precipitate was resuspended in 100 mM NaCl buffer B (50 mM sodium phosphate buffer, pH 7.5, 10 mM EDTA, and 1 mM DTT). The solution was dialyzed against 100 mM NaCl buffer B and then passed over in series Q-Sepharose (Pharmacia), SP-Sepharose (Pharmacia), and Affi-Gel Blue (Bio-Rad) affinity matrixes. The Kp13 protein bound to the Affi-Gel Blue matrix and eluted at approximately 2.5 M NaCl buffer B. For desired purity (>95%), the Affi-Gel Blue purification was repeated. The sample was dialyzed against 100 mM NaCl, 20 mM phosphate buffer, pH 7.5, 0.1 mM EDTA, and 0.1 mM DTT.

NMR Sample Preparation. The Diaflo diafiltration system (Amicon) was used to concentrate the sample. After being concentrated, $^1/_{10}$ volume of D_2O was added, which resulted in the following: 0.7−1.3 mM Kp13 protein, 18 mM sodium phosphate buffer, pH 7.5, 90 mM NaCl, 0.1 mM DTT, and 0.1 mM EDTA. For samples with 100% D_2O as the solvent, a volume of H_2O buffer (18 mM sodium phosphate buffer, pH 7.5, 90 mM NaCl, 0.1 mM DTT, and 0.1 mM EDTA) equivalent to the final amount of D_2O buffer required was evaporated to dryness, resuspended in approximately $^1/_{10}$ the final volume of D_2O, again evaporated to dryness, and then resuspended in 100% D_2O. The Diaflo system was used to perform a buffer exchange into the 100% D_2O buffer.

[1] Abbreviations: AMPCPP, α,β-methyleneadenosine triphosphate; CSI, chemical shift index; DTT, dithiothreitol; EDTA, ethylenediaminetetraacetate; PCR, polymerase chain reaction; NMR, nuclear magnetic resonance; NOESY, nuclear Overhauser effect spectroscopy.

NMR Spectroscopy. All of the NMR spectra were collected at 25 °C on 750 or 600 MHz Varian UnityPlus instruments using triple resonance probes (Varian, 5 mm) equipped with actively shielded pulsed field gradients. Quadrature detection in the indirectly detected dimensions was achieved using the States−TPPI schemes (*18*). The sensitivity-enhanced pulsed field gradient approach was used for the collection of the $^{1}H-^{15}N$ HSQC spectra (*19*−*22*) and all HSQC-based triple resonance experiments in which magnetization is detected on the amide protons (*23*−*26*). Presaturation and spin-lock pulses (*27*) were avoided to reduce saturation and chemical exchange of the amide protons. Suppression of the water signal was achieved mostly by the pulse field gradients used for coherence selection of the desired signals and in some experiments by placing the water signal along the $+Z$ axis immediately prior to acquisition through the use of water-selective flip-back pulses (2.2 ms) and gradients (*28*). Assignments of terminal aliphatic methyl groups and aromatic side chains were confirmed by two appropriately optimized constant time $^{1}H-^{13}C$ HSQC experiments (*29*). The ^{15}N-edited NOESY (*30*, *31*), ^{13}C-edited NOESY (*32*), and the simultaneous ^{15}N,^{13}C-edited NOESY (*33*) experiments were recorded using a 100 ms mixing time and the sensitivity-enhanced method (*20*−*22*). The pulse field gradient HCCH-TOCSY experiment (*34*) was recorded on a D_2O sample with a mixing time of 16 ms, and the center of the ^{1}H frequency was set to 2.7 ppm in both proton dimensions to provide greater resolution.

Several modifications were made to the original sensitivity-enhanced pulse sequences. These modifications include the use of double-adiabatic ^{13}C homonuclear decoupling pulses for the elimination of Bloch−Sigert shifts during the t_1 period (*35*). To enhance sensitivity and resolution and to reduce sample heating, where appropriate, the $^{13}C'$ and $^{13}C_\alpha$ regions were simultaneously decoupled using the double-WURST decoupling scheme (*36*). The ^{1}H chemical shifts were referenced relative to external DSS (2,2-dimethyl-2-silapentane-5-sulfonate). The ^{15}N and ^{13}C chemical shifts were referenced indirectly using the $^{1}H/X$ frequency ratios (*37*).

Data Processing. NMR data were processed using FELIX97 (MSI, San Diego, CA) running on an SGI indigo workstation. Forward linear prediction was used to extend the time domain data in the indirectly detected dimensions. The time domain data were zero-filled to increase the spectral resolution in all dimensions. Phase-shifted skewed sine bell squared apodization functions were used in all three dimensions. Cross-peaks were picked using the automated peak-picking routine available in the FELIX program. Noise peaks and spectral artifacts were then removed manually. Post-acquisition water signal suppression was achieved using a sine bell convolution function (provided in FELIX).

Modeling of the MutY/DNA Complex. The MutY p13 C-terminal structure was constructed using the NMR structure of MutT (*15*) as a template using the following protocol. The ensemble of 15 MutT structures was averaged using AMBER5:CARNAL (*38*), and the result was subjected to 2000 steps of minimization using AMBER5:SANDER (*38*). The RMSD between the minimized structure and the 15 parent structures was calculated to be 1.887 ± 0.219. The minimized MutT structure was read into AMBER5:LEAP (*38*) to provide a set of backbone atom coordinates. The amino acid sequence of MutY p13 was then read into LEAP and threaded onto the MutT coordinates. All missing or inappropriate atoms were replaced, and this MutY coordinate set was written out. The new MutY coordinates were then subjected to another 2000 steps of minimization. At this point MutY NOE restraints between β-strands $\beta1$ and $\beta4$ were used to adjust the alignment of $\beta1$ relative to $\beta4$ in a set of MORASS/rMD (*39*) refinements in which the coordinates of residues 242−350 were fixed and only residues 225−241 were allowed to move. MOLMOL (*40*) was then used to calculate the solvent-accessible surface, which was then painted with a colorized palette of the calculated electrostatic charges due to the amino acid side chains. Upon examination it was quickly apparent which face of the p13 molecule had the correct topology and charge distribution to mate properly with the DNA, and this orientation was manually "docked" onto the MutY p26/DNA complex. The full p26-p13/DNA complex was then subjected to minimization and deemed complete.

RESULTS

Resonance Assignments. Sequence-specific backbone resonance assignments were made by correlating cross-peaks in the HSQC, HNCO, HNCA, HN(CO)CA, HNCACB, and CBCA(CO)NH spectra in the standard manner and were reported earlier (*41*). The side chain resonances were determined using the 3D HCCH-TOCSY experiment. The HNCO (*42*) and (HB)CBCACO(CA)HA (*43*) experiments facilitated the α proton and carbonyl carbon assignments. Resonance assignments for the prolines relied on $C_\alpha(i-1)$ and $C_\beta(i-1)$ connectivities from their $i+1$ residues in the triple resonance experiments, when available, $d_{\alpha N(i,i+1)}$ as well as HCCH-TOCSY and ^{13}C-edited NOE correlations. NOE correlations between proline δ protons and the H_α protons of the previous amino acid were also used, particularly in the two instances of sequential prolines. The resonance assignments are deposited with the BioMagResBank at Wisconsin (*44*) with the accession number 4353.

Secondary Structure and Topology. The chemical shift index method (CSI) has proven to be a useful indicator of secondary structure in proteins (*45*). The CSI-derived secondary structure of the MutY Kp13 domain using the H_α, C_α, C_β, and C' chemical shifts shows well-defined areas of β-strands and α-helices. The secondary structure predicted by the CSI method was largely verified by the intensity patterns in the 100 ms mixing time ^{15}N-edited NOESY data. The NOESY data show strong $d_{\alpha N(i+1)}$ and weak $d_{\alpha N(i,i)}$ correlations in the regions predicted by CSI to be β-strands and strong $d_{NN(i,i+1)}$ and $d_{\alpha N(i,i)}$ NOEs, but weak $d_{\alpha N(i,i+1)}$ NOEs, in the regions predicted to be α-helical. The combined CSI and NOE data correlated well and indicated that two α-helices and five β-strands were present in Kp13.

Interstrand NOEs between β-strands were used to construct two β-sheets. The antiparallel β-strands were connected by strong long-range $d_{\alpha\alpha}$ and weaker $d_{\alpha N}$ and d_{NN} NOEs in the ^{13}C-edited NOE data. Parallel β-strands were connected by medium intensity long-range $d_{\alpha N}$ and weak intensity d_{NN} NOEs. The data indicate the presence of two β-sheets (Figure 1). The largest β-sheet consists of strands $\beta1$, $\beta3$, and $\beta4$ with strand $\beta4$ in the middle, running parallel to strand $\beta1$ but antiparallel to strand $\beta3$. A second smaller β-sheet consists of β-strands $\beta2$ and $\beta5$ in an antiparallel alignment. The fact that strands $\beta1$ and $\beta2$, which are in different sheets,

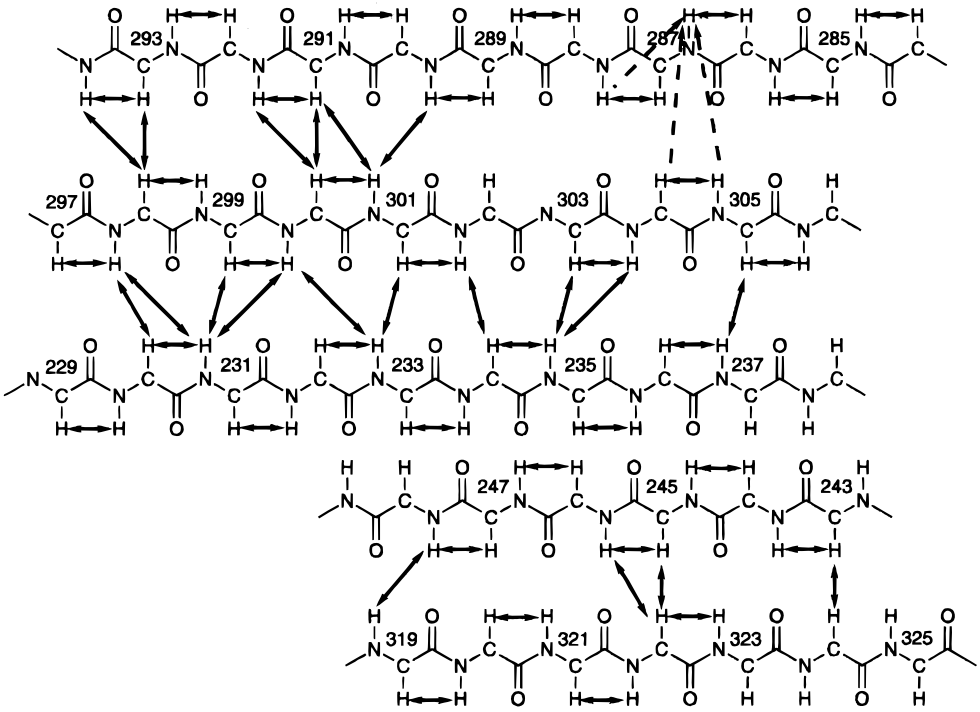

FIGURE 1: Schematic representation of the NOEs used to construct the alignment of the β-strands. Unusual NOEs to the amide proton of L287, which indicate some disruption of the normal β-sheet structure, are indicated by dashed arrows.

```
                          β1          β2
MutY(E. coli)      225    KQTLPERTGYFLLLQHEDEVLLAQRPPSGLWGGLYCFPQFADEES
MutT(E. coli)        1      MKKLQIAVGIIRNENNEIFITRRAADAHMANKLEFPGGKIEMG
                            β1          β2

                          α1                  β3          β4
MutY(E. coli)      270    ------LRQWLAQRQIAADMLTQLTAFRHTFSHFHLDIVPMWLPV
MutT(E. coli)       44    ETPEQAVVRELQEEVGITPQHFSLFEKLEYEFPDRHITLWFWLVE
                            α1                  β3          β4

                                    β5                  α2
MutY(E. coli)      309    --SSFTGCMDEGNALWYNLAQPPSVGLAAPVERLLQQLRTGAPV
MutT(E. coli)       89    RWEGEPWGKEGQPGEWMSLVGLNADDFPPANEPVIAKLKRL
                                    β5                  α2
```

FIGURE 2: Sequence alignment of the *E. coli* MutY C-terminal domain and MutT proteins illustrating the common secondary structural elements present in both proteins. Conserved residues are in bold letters. The underlined residues MutY R271, I279, F294, and H298 and MutT R52, I60, F75, and H79 are conserved in the alignment of ref *13*. See text for an explanation of the differences between the two alignments.

are separated by only five residues suggests that the two β-sheets might be connected, but no definitive connections between these two strands have been determined to date. Another interesting aspect of the larger β-sheet is the unusual NOEs observed between the amide proton of L287 and the amide proton of W305 and the H_α of M304, which indicate some deviation from the normal β-strand structure of β3 near L287. The lack of NOEs observed between the amide proton of Q286, or the α proton of L287, to protons on β-strand β4 further supports such a deviation in structure. However, strong $d_{\alpha N(i,i+1)}$ NOEs were still observed from residues 284−292. MutT has a similar deviation in the planarity of β3 between residues 66 and 68 (*15*).

DISCUSSION

Relationship with MutT. It has recently been suggested that the C-terminal domain of MutY may have evolved from MutT, an 8-oxo-dGTPase (*13*), despite their extremely low sequence identity (~12% with two gaps). The present data strongly agree with this hypothesis. The secondary structure of the MutY p13 domain is essentially the same as that of MutT, although the lengths of the loops connecting secondary elements are slightly different in the two proteins and the length of the first α-helix is three residues shorter in MutY (Figure 2). In addition, the overall topology of the β-sheets in the two proteins is nearly identical, with the only significant difference being that in MutT the two β-sheets were connected by a few NOE correlations.

In the alignment of Figure 2, MutY residues L270 through V308 have been shifted one residue in the N-terminal direction relative to the alignment suggested by Noll et al. (*13*), and the gap between residues V308 and S309 has been increased by one residue. In our manual adjustment to the alignment of Noll et al., MutT residues L54, L67, W85, and L86 are conserved, rather than residues R52, I60, F75, and H79. In the MutT structure, the H_δ protons of L54 in helix α1 interact with the aromatic portion of W85 in strand β4, and the H_α and H_β protons of W85 are less than 3 Å from residue L67 in strand β3. Thus this alignment conserves

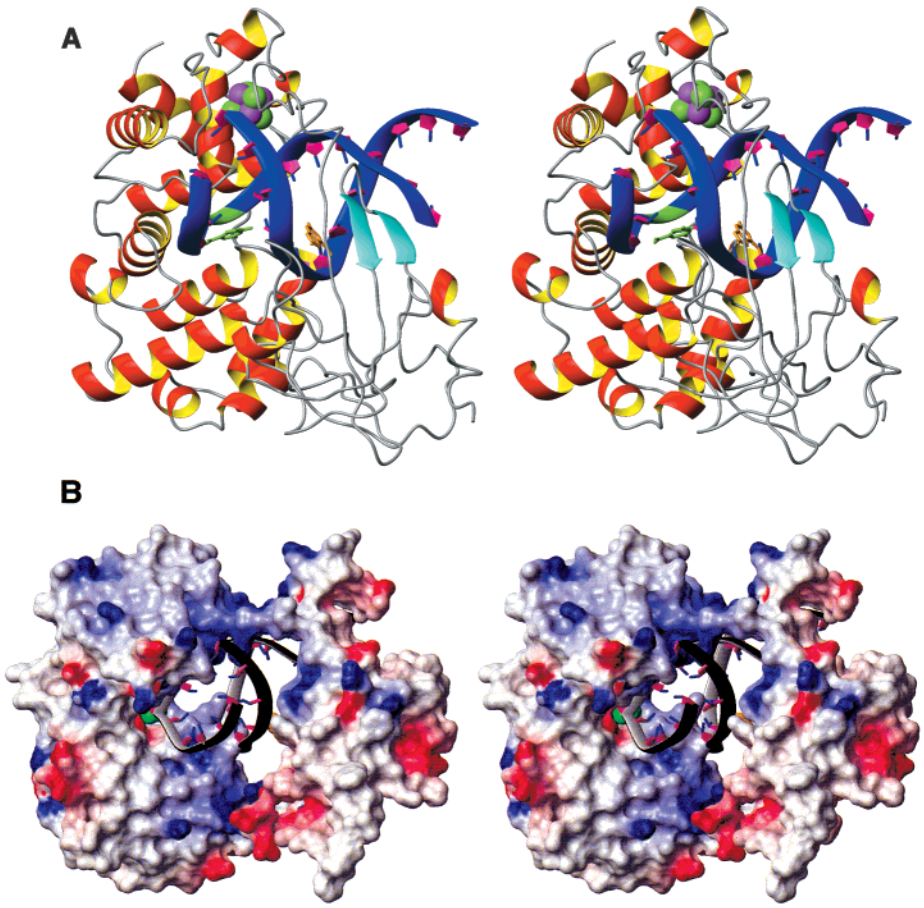

FIGURE 3: (A) Stereoview of a model p13-p26 composite protein with docked DNA. (B) Stereoview of the protein complex showing the electrostatic potential of the residues. The potentials are indicated by blue (positive) and red (negative). The coordinates of the DNA are from an oligonucleotide containing 1-azaribose as an abasic site analogue cocrystallized with AlkA. The positions of the flipped out bases are represented by adenines in the lower right center front (yellow) and in the upper left center (green) of the DNA binding domain in diametric opposition. The structure of the p13 domain was calculated with AMBER 5.0 (*38*) from the NMR secondary structure constraints applied to the MutT structure, and the MutY·DNA model was built by docking the AlkA DNA duplex with the MutY using MIDAS 2.1 (*48*) and rendered with MOLMOL 2.6 (*40*). The position of the 1-azaribose abasic site analogue is rendered in green on a DNA strand. The cubic Fe_4S_4 moiety is rendered in green (Fe) and magenta (S) and is visible near the top in this view.

hydrophobic interactions which appear to be integral to the MutT structure. In addition, MutT residues L54 and L67 have been shown to interact with α,β-methyleneadenosine triphosphate (AMPCPP) and/or dGMP (*46*). This alignment also aligns MutT residue V50, which binds AMPCPP, with MutY residue L270, a conservative substitution. In contrast, the conserved MutT residues R52, I60, F75, and H79 in the Noll alignment do not interact with AMPCPP or dGMP (*43*). The present alignment is also consistent with the NOESY data for p13. The alignment of Noll et al. (*13*) suggests that the H_α protons of p13 residues 294 and 292 in β3 should be directly across the β-sheet from the H_α protons of residues 299 and 301, respectively, in β4. However, the NOESY data indicate that residues 293 and 291 are across from residues 298 and 300, respectively. A similar one-residue shift is observed in the NOESY data between β-strands β1 and β4. Thus, although a total of four residues are conserved between MutY residues 270 and 308 in the present alignment as well as in that of Noll et al. (*13*), which are underlined in Figure 2 for comparison, the present alignment is consistent with the NOESY data for p13 and conserves a cluster of four MutT residues which interact with each other and with substrate analogues.

The similarity between the secondary structure and topology of the C-terminal domain of MutY and MutT strongly supports the hypothesis that the two share a common evolutionary origin. The similarity is surprising considering the sequence identity between the two proteins is only 12%. Our structural results combined with the kinetic analyses of Noll et al. (*13*) strongly support the hypothesis that the C-terminal domain provides a strong determinant of specificity for 8-oxoG.

Speculation on the Role of the p13 Domain. The C-terminal domain of MutY is clearly evolutionarily related to MutT, a pyrophosphohydrolase which recognizes the mutated 8-oxoG base (*14*). While speculative, MutY may recognize the 8-oxoG·A mismatch by a "double flip" mechanism: the p26 catalytic domain recognizes mismatched dA by a single-base base flip mechanism, and the p13 domain similarly recognizes the 8-oxoG by a single-base base flip mechanism on the opposing strand. Noll et al. (*13*) found that the catalytic domain of MutY dissociates from DNA containing 8-oxoG·abasic or G·abasic sites at nearly equal rates but that the full-length MutY enzyme dissociates 1500-fold more slowly. These studies also found a 30-fold faster adenine excision rate for MutYwith 8-oxoG·A mismatches relative to G·A mismatches, and the relative rate dropped to only 4-fold upon deletion of the MutY p13 domain. On the basis of these kinetic data, they suggest that the p13 domain could bind to the 8-oxoG across from the flipped out adenine.

As they note, a flipped out configuration for 8-oxoG would satisfy their kinetic model that "8-oxoG binding destabilize the 8-oxoG-A mismatches and promote the flipping of adenine" (*13*). A recent crystallographic study of *E. coli* endonuclease IV complexed with an oligonucleotide containing an abasic site analogue also reports strong evidence for a double nucleotide flipping mechanism (*47*).

As shown in Figure 3, we have modeled a lesion DNA/MutY complex using the X-ray crystal structure of the p26 domain with bound adenine (*11*), the coordinates of DNA from an AlkA DNA cocrystal structure (*49*), and a model for the p13 domain based upon the NMR data reported here and the published 3D structure of MutT (*15*). The DNA is an oligonucleotide containing the abasic site analogue 1-azaribose in a cocrystal with AlkA whose catalytic domain is homologous to the N-terminal domain of MutY. Positioning one strand containing the flipped A base into the p26 domain still allows the p13 domain to position itself on the opposite side of the mispair, near a putative 8-oxoG binding pocket based on MutT (*15*). Consistent with the hypothesis for a double flip mechanism, both bases of the 8-oxoG·A mispair can be flipped into the corresponding 8-oxoG and A binding pockets. This dual mismatch recognition through nucleotide flipping might provide an explanation for the 8-oxoG·A mismatch specificity.

ACKNOWLEDGMENT

We thank Prof. Tom Ellenberger (Harvard University) for the crystallographic coordinates of the DNA used in the protein/DNA model shown in Figure 3. We also thank Drs. Krishna Rajarathnam and Werner Braun for helpful discussions and suggestions.

REFERENCES

1. Gilchrest, B. A., and Bohr, V. A. (1997) *FASEB J. 11*, 322−330.
2. Tchou, J., and Grollman, A. P. (1993) *Mutat. Res. 299*, 277−287.
3. Shibutani, S., Takeshita, M., and Grollman, A. P. (1991) *Nature 349*, 431−434.
4. Michaels, M. L., and Miller, J. H. (1992) *J. Bacteriol. 174*, 6321−6325.
5. Grollman, A. P., and Moriya, M. (1993) *Trends Genet. 9*, 246−249.
6. Michaels, M. L., Tchou, J., Grollamn, A. P., and Miller, J. H. (1992) *Biochemistry 31*, 10964−10968.
7. Nghiem, Y., Cabrera, M., Cupples, C. G., and Miller, J. H. (1988) *Proc. Natl. Acad. Sci. U.S.A. 85*, 2709−2713.
8. Slupska., M. M., Baikalov, C., Luther, W. M., Chiang, J., Wei, Y., and Miller, J. H. (1996) *J. Bacteriol. 178*, 3885−3892.
9. Manuel, R. C., Czerwinski, E. W., and Lloyd, R. S. (1996) *J. Biol. Chem. 271*, 16218−16226.
10. Gogos, A., Cillo, J. C., Clarke, N. D., and Lu, A. (1996) *Biochemistry 35*, 16665−16671.
11. Guan, Y., Manual, R. C., Arvai, A. S., Parikh, S. S., Mol, C. D., Miller, J. H., Lloyd, R. S., and Tainer, J. A. (1998) *Nat. Struct. Biol. 5*, 1058−1064.
12. Manual, R. C., and Lloyd, R. S. (1997) *Biochemistry 36*, 11140−11152.
13. Noll, D. A., Gogos, A., Granek, J. A., and Clarke, N. D. (1999) *Biochemistry 38*, 6374−6379.
14. Maki, H., and Sekiguchi, M. (1992) *Nature 355*, 273−275.
15. Abeygunawardana, C., Weber, D. J., Gittis, A. G., Frick, D. N., Lin, J., Miller, A., Bessman, M. J., and Mildvan, A. S. (1995) *Biochemistry 34*, 14997−15005.
16. Michaels, M. L., Pham, L., Nghiem, Y., Cruz, C., and Miller, J. H. (1990) *Nucleic Acids Res. 18*, 3841−3845.
17. Belagaje, R. M., Reams, S. G., Ly, S. C., and Prouty, W. F. (1997) *Protein Sci. 6*, 1953−1962.
18. Marion, D., Ikura, M., Tschudin, R., and Bax, A. (1989) *J. Magn. Reson. 85*, 393−399.
19. Bax, A., and Pochapsky, S. S. (1992) *J. Magn. Reson. 99*, 638−643.
20. Kay, L. E., Keifer, P., and Saarinen, T. (1992) *J. Am. Chem. Soc. 114*, 1063−1065.
21. Schleucher, J., Sattler, M., and Griesinger, C. (1993) *Angew. Chem., Int. Ed. Engl. 32*, 1489−1491.
22. Muhandiram, D. R., and Kay, L. E. (1994) *J. Magn. Reson. B103*, 203−216.
23. Kay, L. E., Ikura, M., Tschudin, R., and Bax, A. (1990) *J. Magn. Reson. 89*, 496−514.
24. Grzesiek, S., and Bax, A. (1992) *J. Magn. Reson. 96*, 432−440.
25. Grzesiek, S., and Bax, A. (1993) *J. Am. Chem. Soc. 115*, 12593−12594.
26. Wittekind, M., and Mueller, L. (1993) *J. Magn. Reson. B101*, 201−205.
27. Messerle, B. A., Wider, G., Otting, G., Weber, C., and Wuthrich, K. (1989) *J. Magn. Reson. 85*, 608−613.
28. Grzesiek, S., and Bax, A. (1993) *J. Biomol. NMR 3*, 185−204.
29. Vuister, G. W., and Bax, A. (1992) *J. Magn. Reson. 98*, 428−435.
30. Marion, D., Kay, L. E., Sparks, S. W., Torchia, D. A., and Bax, A. (1989) *J. Am. Chem. Soc. 111*, 1515−1517.
31. Zuiderweg, E. R. P., and Fesik, S. W. (1989) *Biochemistry 28*, 2387−2391.
32. Ikura, M., Kay, L. E., Tschudin, R., and Bax, A. (1990) *J. Magn. Reson, 86*, 204−209.
33. Pascal, S. M., Muhandiram, D. R., Yamazaki, T., Forman-Kay, J. D., and Kay, L. E. (1994) *J. Magn. Reson. B103*, 197−201.
34. Kay, L. E., Xu, G. Y., Singer, A. U., Muhandiram, D. R., and Forman-Kay, J. D. (1993) *J. Magn. Reson. B101*, 333−337.
35. Zhang, S., and Gorenstein, D. G. (1998) *J. Magn. Reson. 132*, 81−87.
36. Zhang, S., Wu, J., and Gorenstein, D. G. (1996) *J. Magn. Reson. A123*, 181−187.
37. Live, D. H., Davis, D. G., Agosta, W. C., and Cowburn, D. (1984) *J. Am. Chem. Soc. 106*, 6104−6105.
38. Case, D. A., Pearlman, J. W., Caldwell, T. E., Chetham, T. E., III, Ross, W. S., Simmerling, C. L., Darden, T., Merz, K. M., Stanton, A. L., Cheng, J. J., Vincent, M., Crowley, M., Ferguson, D. M., Radmer, R. J., Seibel, G. L., Singh, U. C., Weiner, P. K., and Kollman, P. A. (1997) AMBER 5.0, University of California, San Francisco.
39. Meadows, R., Post, C. B., Luxon, B. A., and Gorenstein, D. G. (1996) MORASS Program, University of Texas Medical Branch, Galveston.
40. Koradi, R., Billeter, M., and Wuthrich, K. (1996) *J Mol. Graphics 14*, 51−55.
41. Volk, D. E., Thiviyanathan, V., House, P. G., Lloyd, R. S., and Gorenstein, D. G. (1999) *J. Biomol. NMR 14*, 385−386.
42. Ikura, M., Bax, A., Clore, G. M., and Gronenborn, A. M. (1990) *J. Am. Chem. Soc. 112*, 9020−9022.
43. Kay, L. E. (1993) *J. Am. Chem. Soc. 115*, 2055−2057.
44. http://www.bmrb.wisc.edu/.
45. Wishart, D. S., and Sykes, B. D. (1994) *J. Biomol. NMR 4*, 171−180.
46. Frick, D, N., Weber, D. J., Abeygunawardana, C., Gittis, A. G., Bessman, M. J., and Mildvan, A. S. (1995) *Biochemistry 34*, 5577−5586.
47. Hosfield, D. J., Guan, Y., Haas, B. J., Cunningham, R. P., and Tainer, J. A. (1999) *Cell 98*, 397−408.
48. Ferrin, T. E., Huang, C. C., Jarvis, L. E., and Langridge, R. (1988) *J. Mol. Graphics 6*, 13−37.
49. Hollis, T., Ichikawa, Y., and Ellenberger, T. (2000) *EMBO J. 19*, 758−766.

BI000416P